

1 **Precipitation and synoptic regime in two extreme years**  
2 **2009 and 2010 at Dome C, Antarctica – implications for ice**  
3 **core interpretation**

4  
5  
6 **E. Schlosser<sup>1,2</sup>, B. Stenni<sup>3</sup>, M. Valt<sup>4</sup>, A. Cagnati<sup>4</sup>, J. G. Powers<sup>5</sup>, K. W. Manning<sup>5</sup>,**  
7 **M. Raphael<sup>6</sup>, and M. G. Duda<sup>5</sup>**

8  
9 [1] {Inst. of Atmospheric and Cryospheric Sciences, University of Innsbruck,  
10 Innsbruck, Austria}

11 [2] {Austrian Polar Research Institute, Vienna, Austria}

12 [3] {University of Venice, Venice, Italy}

13 [4] {Avalanche Service Arabba, Italy}

14 [5] {National Center for Atmospheric Research, Boulder, CO, USA}

15 [6] {Department of Geography, University of California, Los Angeles, California,  
16 USA}

17  
18  
19  
20  
21 submitted to: Atmospheric Chemistry and Physics

22 18 September 2015

23 revised version for ACPD 13 October 2015

24 revised version after review 10 February 2016

25 re-revised version March 23<sup>th</sup> 2016

26 final version April 7<sup>th</sup> 2016

27  
28  
29 Correspondence to: E. Schlosser ([Elisabeth.Schlosser@uibk.ac.at](mailto:Elisabeth.Schlosser@uibk.ac.at))

## 30 **Abstract**

31

32 At the East Antarctic deep ice core drilling site Dome C, daily precipitation measurements  
33 have been initiated in 2006 and are being continued until today. The amounts and stable  
34 isotope ratios of the precipitation samples as well as crystal types are determined. Within the  
35 measuring period, the two years 2009 and 2010 showed striking contrasting temperature and  
36 precipitation anomalies, particularly in the winter seasons. The reasons for these anomalies  
37 are analysed using data from the mesoscale atmospheric model WRF (Weather Research and  
38 Forecasting Model) run under the Antarctic Mesoscale Prediction System (AMPS). 2009 was  
39 relatively warm and moist due to frequent warm air intrusions connected to amplification of  
40 Rossby waves in the circumpolar westerlies, whereas the winter of 2010 was extremely dry  
41 and cold. It is shown that while in 2010 a strong zonal atmospheric flow was dominant, in  
42 2009 an enhanced meridional flow prevailed, which increased the meridional transport of heat  
43 and moisture onto the East Antarctic plateau and led to a number of high-  
44 precipitation/warming events at Dome C. This was also evident in a positive (negative) SAM  
45 (Southern Annular Mode) index and a negative (positive) ZW3 (Zonal Wave number three)  
46 index during the winter months of 2010 (2009). Changes in the frequency or seasonality of  
47 such event-type precipitation can lead to a strong bias in the air temperature derived from  
48 stable water isotopes in ice cores.

49

50

## 51 **1 Introduction**

52

53 Although Antarctic precipitation has been studied for approximately half a century (see e.g.  
54 Bromwich, 1988), a number of open questions remain. There are two key motivations for  
55 studying Antarctic precipitation. The first is that precipitation/snowfall is the most important  
56 positive component of the mass balance of Antarctica. This is receiving increasing attention in  
57 discussions of climate change since the mass balance response to global warming can  
58 considerably influence sea level change. A possible increase of precipitation in a future  
59 climate due to higher air temperatures and therefore increased saturation vapour pressure  
60 would mean storage of larger amounts of water in the Antarctic ice sheet, thus mitigating sea  
61 level rise (Church et al., 2013). So far, the expected increase in precipitation has not been

62 found in the measurements (e.g. Monaghan et al., 2006). However, in one projection derived  
63 from a combination of various models and ice core data, Frieler et al. (2015) stated a possible  
64 increase in Antarctic accumulation on the continental scale of approximately 5% K<sup>-1</sup>. In some  
65 parts of Antarctica, higher accumulation would lead to increased ice flow and thus dynamical  
66 ice loss, which would reduce the total mass gain (Winkelmann et al., 2012; Harig and Simons,  
67 2015). Thus, for modelling and calculation of the Antarctic mass balance, precipitation  
68 amounts and precipitation regimes have to be known as exactly as possible.

69 A second driver for studying Antarctic precipitation is that the ice of Antarctica is an  
70 unparalleled climate archive: ice cores up to 800.000 years old yield crucial information about  
71 palaeotemperatures and the past constitution of the atmosphere (e.g. EPICA community  
72 members, 2004). To derive former air temperatures from ice cores, the stable-isotope ratios of  
73 water are used primarily. A linear spatial relationship has been found between mean annual  
74 stable isotope ratios in Antarctic precipitation and annual mean air temperature at the  
75 deposition site although the isotope ratios depend in a complex way on mass-dependent  
76 fractionation processes during moisture transport and precipitation formation (Dansgaard,  
77 1964). This spatially derived linear relationship has been found not to hold temporally,  
78 however (Jouzel et al., 2003; Jouzel, 2014). Apart from air temperature, several other factors  
79 influence the stable isotope ratio, such as seasonality of precipitation, location of and  
80 conditions at the moisture sources and conditions along moisture transport paths (e.g. Noone  
81 et al., 1999; Schlosser, 1999; Jouzel et al., 2003; Sodemann et al., 2008; Sodemann and Stohl,  
82 2009, ). Thus, for a correct interpretation of the ice core data a thorough understanding of the  
83 atmospheric processes responsible for the precipitation is needed, as it was the precipitation  
84 that ultimately formed the glacier ice investigated in the cores. In particular, information  
85 about precipitation mechanisms, moisture sources and transport paths, and atmospheric  
86 conditions at the final deposition site is required.

87 Measuring Antarctic precipitation is a challenge, not only due to the remoteness and extreme  
88 climate of the continent, but also due to difficulties in distinguishing between drifting/blowing  
89 snow and falling precipitation. The latter is due to the high wind speeds that typically  
90 accompany precipitation events in coastal areas. In the interior of the continent, while wind  
91 speeds are lower than at the coast, the threshold for drifting snow is often lower due to lower  
92 snow densities as well. Measurements are also complicated by the extremely small amounts  
93 of precipitation produced in the cold and dry air. Precipitation measurements with optical  
94 devices may hold some hope for improved data in the future, but these instruments are

95 currently in the testing phase in Antarctica (Colwell, pers. comm.). In light of the lack of  
96 observations, atmospheric models have become increasingly useful tools to investigate  
97 Antarctic precipitation (Noone and Simmons, 1998; Noone et al., 1999; Noone and Simmons,  
98 2002; Bromwich et al., 2004; Schlosser et al., 2008, 2010a; 2010b; ).

99 This study focusses on the differences in the precipitation regime of two contrasting years  
100 within the short measuring period, motivated by the consequences different precipitation/flow  
101 regimes have on stable isotope interpretation. The present investigation concentrates on the  
102 years 2009 and 2010. These years were chosen because they showed striking contrasting  
103 temperature and precipitation anomalies, particularly in the winter seasons. Fogt (2010)  
104 reported that temperatures in the Antarctic were persistently above average in the mid-to-  
105 lower troposphere during the winter of 2009. The positive surface temperature anomalies  
106 were most marked in East Antarctica. In 2010, the picture was very different from 2009, with  
107 generally below-average temperatures on the East Antarctic plateau in winter and spring  
108 (Fogt, 2011).

109

110

## 111 **2 Study site**

112 Dome C (75.106 °S, 123.346 °E, elevation 3233m) is one of the major domes on the East  
113 Antarctic ice sheet. Its mean annual temperature is -54.5 °C, and the mean annual  
114 accumulation derived from ice cores amounts to 25 mm water equivalent (w.e.)/yr. Several  
115 deep ice cores have been retrieved at Dome C, the first one in 1977/78, reaching a depth of  
116 906 m, corresponding to an age of approximately 32,000 yr. The thermally drilled core was  
117 retrieved during the International Antarctic Glaciological Project (Lorius et al., 1979).

118 The oldest ice to date has been obtained at Dome C through the European deep drilling  
119 project EPICA (European Project for Ice Coring in Antarctica). The drilling was completed in  
120 January 2006; at the base of the 2774.15 m long ice core the age of the ice was estimated to be  
121 800.000 yr, thus covering eight glacial cycles (EPICA community members, 2004). To  
122 support the EPICA drilling operation, the French-Italian Antarctic wintering base Dome  
123 Concordia became operational in 2005.

124

125

### 126 **3 Previous work**

127 Precipitation conditions in the interior of Antarctica are very different from those in coastal  
128 areas. Whereas precipitation at the coast is usually caused by frontal systems of passing  
129 cyclones that form in the circumpolar trough (e.g. Simmonds et al., 2002), in the interior  
130 different precipitation mechanisms are at play. On the majority of days, only diamond dust,  
131 also called clear-sky precipitation, is observed. It forms due to radiative cooling in a nearly  
132 saturated air mass. Although diamond dust is predominant temporally, it does not necessarily  
133 account for the largest fraction of the total yearly precipitation. It has been shown that a few  
134 snowfall events per year can bring up to 50% of the total annual precipitation (Braaten et al.,  
135 2000; Reijmer and van den Broeke, 2003; Fujita and Abe, 2006; Schlosser et al., 2010a;  
136 Gorodetskaya et al., 2013). Those events are due to amplification of Rossby waves in the  
137 circumpolar westerlies, which increases the meridional transport of heat and moisture  
138 polewards. In extreme cases this can even mean a transport from the Atlantic sector across the  
139 continent to the Pacific side (Sinclair, 1981; Schlosser et al., 2015b) The relatively moist and  
140 warm air is orographically lifted over the ice sheet, followed by cloud formation and/or  
141 precipitation (Noone et al, 1999; Massom et al., 2004; Birnbaum et al., 2006; Schlosser et al.,  
142 2010). Except for the study by Fujita and Abe (2006), all of these investigations were based  
143 on model and Automatic Weather Station (AWS) data, rather than daily precipitation  
144 measurements.

145 For a long time it was believed in ice core studies that precipitation represented in Antarctic  
146 ice cores is formed close to the upper boundary of the temperature inversion layer assuming  
147 that the largest moisture amounts are found where the air temperature is highest (Jouzel and  
148 Merlivat, 1984). This is a very simplified view that is, however, widely used in ice core  
149 studies. It assumes that there are basically no multiple temperature inversions and that  
150 humidity is only dependent on temperature through the Clausius-Clapeyron equation, which  
151 describes the temperature dependence of vapour pressure. This would mean that humidity and  
152 temperature inversions would always have a similar profile. However, more recent studies  
153 have shown that humidity inversions are parallel to the temperature inversion only in 50% of  
154 the cases, and often multiple humidity (and temperature) inversions occur (Nygard et al.,  
155 2013). In particular, the local cycle of sublimation and re-sublimation (deposition) is poorly  
156 known, but it is important for both mass balance and isotope fractionation studies.

157 At Dome Fuji, at an elevation of 3810m, the air can be so dry that, in spite of the advection of  
158 warm and moist air related to amplified Rossby waves, no precipitation is observed at the site.

159 However, this synoptic situation can cause a strong warming in the lower boundary layer  
160 (particularly during blocking situations) due to a combination of warm air advection and  
161 removal of the temperature inversion layer by increased wind speed that induces mixing and  
162 cloud formation, which in turn increases downwelling longwave radiation (Enomoto et al.,  
163 1998; Hirasawa et al., 2000). Increased precipitation amounts can also be observed after a  
164 snowfall event when the warm air advection has ended, but increased levels of moisture  
165 prevail, which can lead to extraordinarily high amounts of diamond dust precipitation  
166 (Hirasawa et al., 2013). In West Antarctica, intrusions of warm, marine air can lead to  
167 increased cloudiness, precipitation and air temperature. A change in the frequency or intensity  
168 of such warm air intrusions could have a large effect on West Antarctic climate if the mean  
169 general circulation changed (Nicolas and Bromwich, 2011).

170 Moisture origin has been investigated in various studies using back-trajectory calculations  
171 employing different models and methods (Reijmer et al., 2002; Sodemann et al. 2008; Suzuki  
172 et al., 2008; Sodemann and Stohl, 2009; Scarcilli et al., 2010; ;). In a recent study by  
173 Dittmann et al. (2015), who investigated precipitation and moisture sources at Dome F for  
174 precipitation events in 2003, it was estimated that the origin of the moisture was farther south  
175 (on average at 50°S) and the transport occurred lower in the atmosphere) than previously  
176 assumed in ice core studies (Masson-Delmotte et al., 2008).

177 Dome C is a deep ice core drilling site. However, the measurements presented here are the  
178 first derived from fresh snow samples at this site. A similar study, if only for a period of  
179 approximately one year, was carried out by Fujita and Abe (2006) at Dome Fuji (see Fig. 1),  
180 another deep-drilling site in East Antarctica. They investigated daily precipitation data  
181 together with measurements of stable isotope ratios of the precipitation samples. Temporal  
182 variations of  $\delta^{18}\text{O}$  were highly correlated with air temperature. Half of the annual  
183 precipitation resulted from only 11 events (18 days), without showing any seasonality. The  
184 other half was due to diamond dust. Similar results were found in studies by Schlosser et al.  
185 (2010a), at Kohnen Station (see Fig. 1) and by Reijmer and Van den Broeke (2003), who used  
186 data from automatic weather stations in Dronning Maud Land. The precipitation-weighted  
187 temperature was significantly higher than the mean annual surface temperature because the  
188 precipitation events were related to warm-air advection, which leads to a warm bias in the  
189  $\delta^{18}\text{O}$  record.

190

## 191 **4 Data and methods**

### 192 **4.1 Precipitation**

193 Daily precipitation measurements were initiated at Dome C in 2006, and have, with some  
194 interruptions, been continued until today. Daily precipitation amounts are measured using a  
195 wooden platform set up at a distance of 800 m from the main station, at a height of 1 m above  
196 the snow surface to avoid contributions from low drifting snow. For the same reason, the  
197 platform is surrounded by a rail of approximately 8 cm height. The measurements include  
198 precipitation sampling and analysis of stable water isotopes ( $\delta^{18}\text{O}$ ,  $\delta\text{D}$ ) of the samples.  
199 Additionally, the crystal structure of the precipitation is analysed in order to distinguish  
200 between diamond dust, snowfall, and drift snow. Diamond dust consists of extremely fine ice  
201 needles whereas synoptic snowfall shows various types of regular snow crystals, which tend  
202 to be broken in case of drifting/blowing snow. The snow crystal type depends on air  
203 temperature during formation in the cloud. Samples of mixed crystal types can also occur.

204 While errors of the precipitation measurements cannot be quantified, it is understood that they  
205 can exceed 100% given the extremely small precipitation amounts.

206 The Dome C precipitation series is the first and so far only multi-year precipitation/stable  
207 isotope series at an Antarctic deep ice core drilling site.

208

### 209 **4.2 AWS data**

210 The Antarctic Meteorological Research Center (AMRC) and Automatic Weather Station  
211 (AWS) Program are sister projects of the University of Wisconsin-Madison funded under the  
212 United States Antarctic Program (USAP) that focus on data for Antarctic research support,  
213 providing real-time and archived weather observations and satellite measurements and  
214 supporting a network of automatic weather stations across Antarctica.

215 The current AWS at Dome C was set up by the AMRC, in December 1995. The station  
216 measures the standard meteorological variables of air temperature, pressure, wind speed, wind  
217 direction, and humidity. Data can be obtained from <http://amrc.ssec.wisc.edu>. Note that an  
218 initial AWS (named Dome C) had been set up in 1985, however, at a distance of about 70 km  
219 from the current site. Thus, only data from the new station (Dome C II) are used in the present  
220 study.

### 222 **4.3 WRF Model Output from the AMPS Archive**

223 In addition to the observations described above, this study uses numerical weather prediction  
224 (NWP) model output for analysis of the synoptic environments of the target years, of  
225 precipitation processes, and of events. The output is from forecasts of the Weather Research  
226 and Forecasting (WRF) Model (Skamarock et al., 2008) run under the Antarctic Mesoscale  
227 Prediction System (AMPS) (Powers et al., 2003; 2012), a real-time NWP capability that  
228 supports the weather forecasting for the United States Antarctic Program (USAP). The (U.S.)  
229 National Center for Atmospheric Research (NCAR) has run AMPS since 2000 to produce  
230 twice-daily forecasts covering Antarctica with model grids of varying resolutions. The AMPS  
231 WRF forecasts have been stored in the AMPS Archive and used extensively in studies (e.g.  
232 Monaghan et al., 2005; Schlosser et al., 2008; Seefeldt and Cassano, 2008; Seefeldt and  
233 Cassano, 2012). For 2009 and 2010, the WRF output over the Dome C region reflects a  
234 forecast domain with a horizontal grid spacing of 15 km, employing 44 vertical levels  
235 between the surface and 10 hPa. This 15-km grid was nested within a 45-km grid covering  
236 the Southern Ocean, and Fig. 2 shows these domains.

237 Model output from AMPS has been verified through various means over the years. Multi-  
238 year AMPS forecast evaluations have been conducted (Bromwich et al., 2005), and WRF's  
239 ability for the Antarctic in particular has been confirmed (Bromwich et al., 2013). AMPS's  
240 and WRF's Antarctic performance has also been documented in a number of case and process  
241 studies (e.g. Nigro et al., 2011; 2012; Powers, 2007; Bromwich et al., 2013). For model  
242 development within AMPS, verification for both warm and cold season periods is performed  
243 prior to changes in model versions or configurations (Powers et al., 2012). The reliability of  
244 AMPS WRF forecasts is also reflected in their demand from international Antarctic  
245 operations and field campaign forecasting efforts (see e.g. Powers et al., 2012). Lastly,  
246 similarly to how it is used here, AMPS output has been a key tool in previous published  
247 studies of Antarctic precipitation related to ice core analyses (Schlosser et al., 2008; 2010a;  
248 2010b).

249 In this study the WRF output from the AMPS archive is used to study both the synoptic  
250 patterns/general atmospheric circulation and the local conditions related to the precipitation  
251 regimes and events in the years compared. The WRF forecasts provide reliable depictions of  
252 conditions and their evolution.



## 254 **5 Results**

### 255 **5.1 Temperature and precipitation**

256 Figure 3a shows the mean monthly air temperature observed at the Dome C AWS for 2009  
257 and 2010 as well as the mean of 1996-2014. The mean annual cycle exhibits the typical  
258 coreless winter (van Loon, 1967) with a distinct temperature maximum in summer  
259 (December/January), which has no counterpart in winter, where the months May to August  
260 show relatively similar values. This is due to a combination of the local surface radiation  
261 balance and warm air intrusions. During the first part of the polar night, with the lack of short-  
262 wave radiation, an equilibrium of downwelling and upwelling longwave radiation is reached;  
263 advection of relatively warm air from lower latitudes further reduces the possibility for  
264 cooling. Thus the temperature does not decrease significantly after May (Schwerdtfeger 1984;  
265 King and Turner, 1997).

266 While during the summer months little difference is seen between 2009 and 2010 the winter  
267 months are strikingly different. The lowest mean July temperature of the station record occurs  
268 in 2010 with a value of  $-69.7\text{ }^{\circ}\text{C}$ . This is the lowest monthly mean ever observed at Dome C,  
269  $5.9\text{ }^{\circ}\text{C}$  lower than the average 1996-2014, corresponding to a deviation of  $1.7\sigma$ ,  $\sigma$  being the  
270 standard deviation. In contrast, the highest July mean temperature is found in 2009; with a  
271 value of  $-54.9\text{ }^{\circ}\text{C}$ , it was  $8.9\text{ }^{\circ}\text{C}$  higher (corresponding to  $2.5\sigma$ ) than the long-term July mean  
272 and the only July mean that exceeded  $-60\text{ }^{\circ}\text{C}$ . In Figure 3b, observed daily mean temperatures  
273 and daily precipitation sums for the years 2009 and 2010 are displayed. Again, the differences  
274 between the two years are most striking in winter. In 2009, the temperature variability is very  
275 high, and several warming events with temperatures up to almost  $-30\text{ }^{\circ}\text{C}$  can be seen.  
276 Minimum temperatures are rarely lower than  $-70\text{ }^{\circ}\text{C}$  whereas in 2010, minima are close to  $-80$   
277  $^{\circ}\text{C}$ . The highest temperature in the winter of 2010 was only slightly above  $-50\text{ }^{\circ}\text{C}$ . The winter  
278 2009 thus was not only a “coreless winter”, but had a “warm” core due to the high number of  
279 warm air intrusions.

280 A very high precipitation value of 1.36 mm was measured on 9 February 2010, followed by  
281 0.67 mm on 10 February, both classified as diamond dust from the photographic crystal  
282 analysis.. Considering the extremely low density of diamond dust, a diamond dust amount of  
283 more than 1mm/day at first, seemed to be unlikely. However, the model data do show a

284 precipitation event connected to warm air advection from the north (see below) for this day,  
285 which would indicate the occurrence of snowfall rather than diamond dust. Most likely a  
286 mixture of crystal types was found during this event with the diamond dust on top of the snow  
287 crystals, which possibly led to the classification of the event as diamond dust. (Note that the  
288 crystal classification was carried out purely from photographs by an expert at the Avalanche  
289 Institute in Italy and that snow crystals are also comparatively small at the temperatures  
290 prevailing at Dome C). Also, it was found that increased amounts of diamond dust can prevail  
291 after snowfall events when humidity is still increased compared to the average, but not large  
292 enough to cause real snowfall. The precipitation totals for May to September are 12.0 mm  
293 w.e. for 2009 and 4.3 mm w.e. for 2010. Daily sums exceed 0.25 mm only three times in  
294 2010, but 16 times in 2009. Usually, high daily precipitation amounts are associated with  
295 relative maxima in air temperature. In general, the winter of 2010 was cold and dry, whereas  
296 2009 was relatively warm and moist compared to the long-term average.

297 Figure 4a shows monthly precipitation amounts for 2009 and 2010, distinguishing between  
298 diamond dust, hoar frost, and snowfall; Figure 4b gives the relative frequencies of the three  
299 different observed types of precipitation for both years. Again, large differences between 2009  
300 and 2010 are found. While approximately half of the precipitation fell as snow in 2009, less  
301 than a quarter of the total precipitation stemmed from snowfall in 2010, when mostly diamond  
302 dust was observed. As seen before, the winter months of May to September exhibit the  
303 largest differences. In particular, the extremely “warm” July of 2009 brought high amounts of  
304 snowfall. The lowest amounts of precipitation are seen in austral summer 2009/2010, with no  
305 precipitation observed in November and only very small amounts in December and January.

306 The total amount of precipitation measured on the raised platform is 16.5 mm w.e. for 2009  
307 and 13.4 mm w.e. for 2010, compared to the mean annual accumulation of 25 mm w.e.  
308 derived from firn core and stake measurements (Frezzotti et al., 2005). From the available  
309 data it cannot be determined whether the difference is due to snow removed from the  
310 measuring platform by wind or sublimation or snow added to the snow surface at the stake  
311 array by wind (blowing or drifting snow) or deposition (re-sublimation).

312

## 313 **5.2 Atmospheric flow conditions**

### 314 **5.2.1 Synoptic analyses with AMPS archive data**

315 The synoptic situations that caused precipitation at Dome C were analysed using WRF output  
316 data from the AMPS archive. In particular, fields of 500hpa geopotential height and 24-h  
317 precipitation were used. For the 500hPa geopotential height information the 12-h forecast was  
318 utilized. For 24-h precipitation, the 12-36h forecast sums of precipitation (rather than 0-24h)  
319 were used to allow for model spin up of clouds and microphysical fields. This is considered  
320 long enough for moist process spin-up, but avoids error growth reflected in longer forecast  
321 times (Bromwich et al., 2005).

322 For all precipitation events with observed daily sums exceeding 0.2mm, the synoptic  
323 situations that caused the precipitation were investigated. In total, 29 events were studied, 20  
324 in 2009 and 9 in 2010. For 2009 (2010), the model showed precipitation at Dome C in 44%  
325 (50%) of the studied cases and precipitation in the vicinity in 33 (25) % of the cases; no  
326 precipitation was shown in the model in 22 (25) % of the cases. In total, approximately half of  
327 the precipitation events were represented well by the model, one quarter showed synoptic  
328 events that did not bring precipitation exactly at the location and time of the measurements,  
329 and one quarter of the cases were not forecast by the model at all. An exact quantitative  
330 analysis of the model skill using the entire data series starting in 2006 is ongoing and the  
331 results will be more meaningful than those of only two, not very typical, years.

332 Generally, snowfall events were found to be associated with an amplification of the Rossby  
333 waves in the circumpolar westerlies, which causes a northerly flow across the Dome C region  
334 between a trough to the west and an upper-level ridge to the east of Dome C. This northerly  
335 flow brings relatively warm and moist air from as far as 35 °S - 40 °S to the East Antarctic  
336 plateau, leading to orographic precipitation when it is forced to ascend on the way from the  
337 coast to the high-altitude interior. Variations of this general situation are due to the duration of  
338 the flow pattern (e.g. whether there is a blocking anticyclone or not) and the strength of the  
339 upper-level ridge, which determines how far north the main moisture origin is situated. Figure  
340 5 shows an example of this synoptic situation typical for snowfall events. In the 500hPa  
341 geopotential height field (Fig. 5a) for 13 September 2009 the amplified ridge that leads to a  
342 northerly flow towards Dome C can be seen slightly east of Dome C, with an axis tilted in a  
343 NE-SW direction. Figure 5b displays the 24-h precipitation caused by the N-NE flow onto the  
344 continent. Dome C is situated at the southeastern edge of the precipitation area.

345 A frequent occurrence of the synoptic situation described (as it was the case in 2009) means a  
346 more northern mean moisture source than on average, which has to be taken into account for  
347 deriving air temperature from stable isotopes. (A detailed study using trajectory calculations

348 for all observed precipitation events at Dome C is ongoing.) It was also found to be typical for  
349 precipitation events at Dome C that the main westerly flow is split into a northern branch that  
350 remains zonal, whereas the southern branch starts meandering with a strong meridional  
351 component. This is observed more often at Dome C than at Dome F (Dittmann et al., 2015) or  
352 at Kohnen Station (Schlosser et al., 2010a).

353 Figure 6 presents an example for a case with no precipitation in the model, but relatively large  
354 observed precipitation amounts. The 500hPa geopotential height field (Fig. 6a) shows a  
355 cutoff-high west of Dome C on the day after the precipitation event shown in Figure 5. The  
356 remaining atmospheric moisture is not sufficient to produce precipitation in the model (Fig.  
357 6b), but it does lead to remarkably high amounts of diamond dust and/or hoar frost (0.7 mm  
358 observed during this event). This synoptic situation was also found by Hirasawa et al. (2013)  
359 in a detailed study of the synoptic conditions and precipitation during and after a blocking  
360 event at Dome Fuji. (Note that neither diamond dust nor hoar frost formation is specifically  
361 parameterized in the model.) In 2010, the flow was mainly zonal and the synoptic situations  
362 described above were much less frequent than in 2009 and not as strongly developed.

363 Using the WRF output, monthly mean fields of 500hPa-geopotential height were calculated to  
364 compare the general flow conditions in 2009 and 2010. Figure 7 shows the composite mean  
365 500-hPa geopotential height for July 2009 and 2010, respectively. Even in the monthly mean,  
366 the distinct upper-level ridge in 2009 that projects onto the East Antarctic plateau and leads to  
367 warm air advection and increased precipitation at Dome C is clearly seen.

368 In 2010, in the monthly average, the flow was mainly zonal, which reduced the meridional  
369 exchange of heat and moisture, thus leading to lower temperatures and less precipitation in the  
370 interior of the Antarctic continent.

371

## 372 **5.2.2 Southern Annular Mode**

373 The occurrence of high-precipitation events on the Antarctic plateau due to amplification of  
374 Rossby waves is often connected to a strongly positive phase of the Southern Annular Mode  
375 (SAM). The SAM is the dominant mode of atmospheric variability in the extratropical  
376 Southern Hemisphere. It is revealed as the leading empirical orthogonal function in many  
377 atmospheric fields (e.g. Thompson and Wallace, 2000), such as surface pressure, geopotential  
378 height, surface temperature, and zonal wind (Marshall, 2003). Since pressure fields from

379 global reanalyses commonly used to study the SAM are known to have relatively large errors  
380 in the polar regions, Marshall (2003) defined a SAM index based on surface observations. He  
381 calculated the pressure differences between 40 °S and 65 °S using data from six mid-latitude  
382 stations and six Antarctic coastal stations to calculate the corresponding zonal means. A large  
383 (small) meridional pressure gradient corresponds to a positive (negative) SAM index. The  
384 positive index means strong, mostly zonal westerlies and comparatively little exchange of  
385 moisture and energy between middle and high latitudes, which leads to a general cooling of  
386 Antarctica, except for the Antarctic Peninsula that projects into the westerlies. A negative  
387 SAM index is associated with weaker westerlies and a larger meridional flow component.

388 Figure 8 shows the monthly mean SAM index for 2009 and 2010 (data can be found at  
389 <http://www.nerc-bas.ac.uk/icd/gjma/sam.html>). Whereas in the winter months (May to  
390 September) of 2009 the SAM index was generally negative (with the exception of a weakly  
391 positive value in June), 2010 has positive indices from April to August, with strongly positive  
392 values in June and July, and only a weakly negative index in September. This is consistent  
393 with the pattern of a strong zonal flow with few precipitation events at Dome C due to  
394 amplified ridges in the winter of 2010, with the opposite situation holding in 2009. The  
395 highest SAM index is found in November 2010; however, in austral summer the relationship  
396 between the SAM index and precipitation seems to be less straightforward. The differences  
397 between 2009 and 2010 are not extraordinarily high compared to other years (e.g. 2001/2002  
398 as seen at <http://www.nerc-bas.ac.uk/public/icd/gjma/newsam.spr.pdf>), however, qualitatively  
399 they are in agreement with the observed flow pattern. Furthermore, it should be kept in mind  
400 that SAM explains only about one third of the atmospheric variability in the Southern  
401 Hemisphere (Marshall, 2007) and that the SAM index alone gives no information about the  
402 location of respective ridges and troughs in a highly meridional flow pattern.

403

### 404 **5.2.3 Zonal wave number 3**

405 Another method to investigate the general atmospheric flow conditions is to analyse spatial  
406 and temporal variations of the quasi-stationary zonal waves in the Southern Hemisphere. In  
407 this study zonal wave number 3 (ZW3) is used. While the atmospheric circulation in the  
408 Southern Hemisphere appears strongly zonal (or symmetric), there is a significant non-zonal  
409 (asymmetric) component and ZW3 represents a significant proportion of this asymmetry. It is  
410 a dominant feature of the circulation on a number of different time scales (e.g. Karoly, 1989),

411 is responsible for 8% of the spatial variance in the field (van Loon and Jenne, 1972), and  
412 contributes significantly to monthly and interannual circulation variability (e.g. Trenberth and  
413 Mo, 1985; Trenberth, 1990). The asymmetry is revealed when the zonal mean is subtracted  
414 from the geopotential height field thereby creating a coherent pattern of zonal anomalies, with  
415 the flow associated with these patterns becoming apparent. ZW3 has preferred regions of  
416 meridional flow, which influence the meridional transport of heat and moisture into and out of  
417 the Antarctic. Raphael (2004) defined an index of ZW3 based on its amplitude (effectively the  
418 size of the zonal anomaly) at 50°S showing that ZW3 has identifiable positive and negative  
419 phases associated with the meridionality of the flow. A positive value for this index indicates  
420 more meridional flow (large zonal anomaly) and a negative value more zonal flow (small  
421 zonal anomaly). Note that the ZW3 index used here does not fully capture the shift in phase of  
422 the wave. However, Raphael (2004) found that the net effect is a small reduction in the  
423 amplitude of the wave, but the sign of the index is not influenced. A new approach for  
424 identifying Southern Hemisphere quasi-stationary planetary wave activity that allows  
425 variations of both wave phase and amplitude is described in a recent study by Irving and  
426 Simmonds (2015).

427 Figure 9a shows the monthly mean ZW3 index for the period 2009–2010. From June to  
428 September 2009 the ZW3 index was largely positive except for a comparatively small  
429 negative excursion in July. On the contrary, from June to September 2010 it was negative. The  
430 asymmetry in the circulation suggested by the index is shown in Figure 9b (July 2009) and 9c  
431 (July 2010). These figures were created by subtracting the long-term zonal mean at each  
432 latitude, from the mean 500-hPa geopotential height field in July 2009 and 2010, respectively.  
433 The flow onto Dome C suggested by the alternating negative and positive anomalies is  
434 northerly in July 2009, but has a strong zonal component in July 2010. This information given  
435 by the ZW3 index and the patterns of zonal anomalies is consistent with that suggested by the  
436 SAM.

437

## 438 **6 Discussion and Conclusion**

439 In the present study that was motivated by stable water isotope studies, atmospheric  
440 conditions of the two contrasting years 2009 and 2010 at the Antarctic deep-drilling site  
441 Dome C, on the East Antarctic Plateau were investigated using observational precipitation and  
442 temperature data and data from a mesoscale atmospheric model. The observations from Dome

443 C represent the first and only multi-year series of daily precipitation/stable isotope  
444 measurements at a deep-drilling site, even though “multi” means only nine years in this case.  
445 The differences between the two years 2009 and 2010 were most striking in winter. Whereas  
446 2009 was relatively warm and moist due to frequent warm air intrusions connected to  
447 amplification of Rossby waves in the circumpolar westerlies, the winter of 2010 was  
448 extremely cold and dry, with the lowest monthly mean July temperature observed since the  
449 beginning of the AWS measurements in 1996. This can be explained by the prevailing strong  
450 zonal flow in the winter of 2010, related to a strongly positive SAM index and a negative  
451 ZW3 index. Also, the frequency distribution of the various precipitation types was largely  
452 different in 2009 and 2010, with snowfall prevailing in 2009 whereas diamond dust was  
453 dominant in 2010.

454 Similarly striking differences in weather conditions of 2009 and 2010 were seen in other parts  
455 of East Antarctica. Gorodetskaya et al. (2013) found that accumulation in 2009 was eight  
456 times higher than in 2010 at the Belgian year-round station “Princess Elisabeth”. At this  
457 location, the temperature was also higher in 2009 than in 2010, particularly in fall/early  
458 winter. The findings are supported by Boening et al. (2012), who used observations from  
459 GRACE (Gravity Recovery And Climate Experiment) and found an abrupt mass increase on  
460 the East Antarctic ice sheet in the period 2009-2011. Similarly, Lenaerts et al. (2013)  
461 investigated snowfall anomalies in Dronning Maud Land, East Antarctica. They stated that the  
462 large positive anomalies of accumulation found in 2009 and 2011 stand out in the past  
463 approximately 60 years although comparable anomalies are found further back in time.

464 Distinguishing between the different forms of precipitation, namely diamond dust, hoar frost  
465 and dynamically caused snowfall, is important for both mass balance and ice core  
466 interpretation. For mass balance, the different precipitation types do not have to be known if  
467 the surface mass balance is determined as an annual value from snow pits, firn/ice cores or  
468 stake arrays. For temporally higher resolved precipitation measurements, however, a fraction  
469 of both hoar frost and diamond dust might be just a part of the local cycle of sublimation and  
470 deposition (re-sublimation), thus representing no total mass gain. More detailed  
471 measurements are thus necessary to allow a better understanding of the processes involved.  
472 This also applies to isotopic fractionation during this cycle; continuous measurements of  
473 water vapour stable isotope ratios (e.g. Steen-Larsen et al., 2013) should be included here.

474 For ice core interpretation, the problem generally becomes more complex. Diamond dust is  
475 observed during the entire year without a distinct seasonality. Therefore a signal from an ice

476 core property measured in the ice (in contrast to measured in the air bubbles) will have  
477 contributions from diamond dust that stem nearly equally from all seasons. Although snowfall  
478 events are not very frequent at deep ice core drilling sites, they can account for a large  
479 percentage of the total annual precipitation/accumulation at those locations. If these events  
480 have a seasonality that has changed between glacial and interglacials, a large bias will be  
481 found in the temperature derived from the stable isotopes in ice cores. Today, the frequency of  
482 such snowfall events shows a high inter-annual variability, but both frequency and seasonality  
483 of the events might be different in a different climate due to changes in the general  
484 atmospheric circulation and in sea ice extent (e.g. Godfred-Spenning and Simmonds, 1996).  
485 Since it was found that snowfall events are connected to the synoptic activity in the  
486 circumpolar trough, it is plausible that the seasonality of such events was different during  
487 glacial times because the sea ice edge and the mean position of the westerlies were  
488 considerably farther north than today. This influences the zone of the largest meridional  
489 temperature gradient, thus the largest baroclinicity and consequently cyclogenesis. A larger  
490 sea ice extent might reduce the number of snowfall events in the Antarctic interior in winter  
491 by pushing the zone of largest baroclinicity northwards. However, it is not possible to assess  
492 such hypotheses using observational data since the instrumental period, with few exceptions,  
493 started in Antarctica not before the IGY (International Geophysical Year) 1957/58. However,  
494 modelling studies can be supported by studies of the physical processes in the atmosphere  
495 using recent data, and, in particular, cases of extreme situations can be helpful here. Even if  
496 the full amplitude of the change between glacial and interglacial climates is not observed,  
497 extrema can give insight into the sign and kind of the reaction of the system to a change in  
498 one or several atmospheric variables.

499 Another implication for ice core interpretation derived from the present study is that a more  
500 northern moisture source does not necessarily mean larger isotopic fractionation (which is  
501 usually assumed in ice core studies (e.g. Stenni et al., 2001; 2010). Even without a  
502 quantitative determination of the moisture source it can be said that in an increased meridional  
503 flow, as in 2009, heat and moisture transport from relatively low latitudes is increased, too,  
504 and leads to higher precipitation stemming from more northern oceanic sources than on  
505 average. Although the temperature at the main moisture source is higher than on average for a  
506 more northern moisture source, the depletion in heavy isotopes is comparatively small  
507 because the temperature at the deposition site is also clearly higher than on average due to the  
508 warm air advection, which reduces the temperature difference between the moisture source  
509 region and the deposition site, thus the amount of isotopic fractionation.



510 Looking towards future work, the results here indicate that a combination of process studies  
511 using recent data and modelling of the atmospheric flow conditions on larger time scales will  
512 lead to a better quantitative interpretation of ice core data. Apart from the factors influencing  
513 precipitation itself, it has become clear recently that post-depositional processes between  
514 snowfall events are more important than previously thought because, additionally to processes  
515 within the snowpack, the interaction between the uppermost parts of the snowpack and the  
516 atmosphere is very intense (Steen-Larsen et al., 2013). Parallel measurements of stable  
517 isotope ratios of water vapour and surface snow, combined with meteorological data will give  
518 more insight into these processes in Antarctica.

519 Altogether, this means that, compared to years with predominantly zonal flow (which is the  
520 more frequent situation), in years with enhanced meridional flow (negative SAM index,  
521 positive ZW3 index) higher temperatures and higher amounts of precipitation that is less  
522 depleted of heavy isotopes are expected at Dome C and comparable interior sites in  
523 Antarctica. This is particularly valid for the colder seasons.

524 The relationship between air temperature and stable isotopes of Antarctic precipitation/ice is  
525 anything else but straightforward, since the isotope ratio measured in an ice core (or in the  
526 snow) is the result of a complex precipitation history that is strongly influenced by the  
527 synoptics and general atmospheric flow conditions, followed by post-depositional processes.  
528 Without thorough knowledge of all the processes involved a quantitatively correct derivation  
529 of paleo temperatures from ice core stable water isotopes is thus not possible.

530

### 531 **Author contribution**

532 BS is responsible for the precipitation measurements, MV and AC for the crystal analysis.  
533 MR did the ZW3 study. MD and KW assisted with software development. ES prepared the  
534 manuscript with contributions from JP, KW, MR, and BS.

535

536

### 537 **Acknowledgements**

538 The precipitation measurements at Dome C have been conducted in the framework of the  
539 Concordia station glaciology and ESF PolarCLIMATE HOLOCLIP projects funded in Italy

540 by PNRA-MIUR. This is a HOLOCIP publication number xx. The present study is financed  
541 by the Austrian Science Funds (FWF) under grant P24223. AMPS is supported by the U.S.  
542 National Science Foundation, Division of Polar Programs. We appreciate the support of the  
543 University of Wisconsin-Madison Automatic Weather Station Program with the Dome C II  
544 data set. (NSF grant numbers ANT-0944018 and ANT-12456663). We thank Gareth Marshall  
545 for providing the SAM indices online. We thank all winterers at Dome C, who did the  
546 precipitation sampling. We also thank our editor, Heini Wernli, and Harald Sodemann and  
547 two anonymous reviewers for helpful comments that improved the manuscript.

548

549

550

551

552

553

554

555

556

557

558

559

560

561

562

563

564

565

566

567 **References**

568

569 Birnbaum, G., Brauner, R., and Ries, H.: Synoptic situations causing high precipitation rates  
570 on the Antarctic plateau: observations from Kohnen Station, Dronning Maud Land , Antarctic  
571 Science, 18 (2), pp. 279-288, doi: 10.1017/S0954102006000320, 2006.

572 Boening, C., Lebsock, M., Landerer, F., and Stephens, G. : Snowfall-driven mass change on  
573 the East Antarctic ice sheet. Geophys. Res. Let., 39, L21501, doi:10.1029/GL053316, 2012.

574 Braaten, D. A.: Direct measurements of episodic snow accumulation on the Antarctic polar  
575 plateau. J. Geophysic. Res., 105, (D9) 10,119-10,128, 2000.

576 Bromwich, D. H: Snowfall in high southern latitudes. Rev. Geophys., 26(1) 149-168, 1988.

577 Bromwich, D. H., Guo, Z., Bai, L., and Chen, Q. : Modeled Antarctic Precipitation. Part I:  
578 Spatial and Temporal Variability, *J. Climate*, **17**, 427–447, 2004.

579 Bromwich, D. H., Monaghan, A. J., Manning, K. W., and Powers, J. G.: Real-time forecasting  
580 for the Antarctic: An evaluation of the Antarctic Mesoscale Prediction System (AMPS), Mon.  
581 Weather Rev., 133, 579-603, 2005.

582 Bromwich, D. H., Otieno, F. O., Hines, K. M., Manning, K. W., and Shilo, E.: Comprehensive  
583 evaluation of polar weather research and forecasting performance in the Antarctic. J.  
584 Geophys. Res., 118, 274–292, doi: 10.1029/2012JD018139, 2013.

585 Church, J.A., et al.: Sea Level Change. In: Climate Change 2013: The Physical Science Basis.  
586 Contribution of Working Group I to the Fifth Assessment Report of the Intergovernmental  
587 Panel on Climate Change (Stocker, T.F., D. Qin, D., G.K. Plattner, G. K., M. Tignor, M.,  
588 Allen, S. K., Boschung, J., Nauels, A., Xia, Y., Bex, V., and Midgley, P. M. (eds.)),  
589 Cambridge University Press, Cambridge, United Kingdom and New York, NY, USA, 2013.

590 Dansgaard, W.: Stable isotopes in precipitation, *Tellus*, XVI (4), 436-468, 1964.

591 Dittmann, A., Schlosser, E., Masson-Delmotte, V., Powers, J. G., Manning, K. W., Werner,  
592 M., and Fujita, K.: Precipitation regime and stable isotopes at Dome Fuji, East Antarctica,  
593 Atmos. Chem. Phys. Discuss., doi:10.5194/acp-2015-1012, in review, 2016. Enomoto et al.,  
594 Winter warming over Dome Fuji, East Antarctica and semiannual oscillation in the  
595 atmospheric circulation. J. Geophysic. Res., 103 (D18), 23,103-23,111, 1998.

596 EPICA community members: 8 Glacial cycles from an Antarctic ice core, *Nature*, 429, 623-  
597 628, doi:10.1038/nature02599, 2004.

598 Fogt, R. L. In: Arndt, D. S., Baringer, M. O., and M. R. Johnson, Eds., *State of the Climate in*  
599 *2009*, 6. Antarctica. Special supplement to *Bull. Am. Meteorol. Soc.*, 91 (7) 125-134, 2010.

600 Fogt, R. L. In: Blunden, J., Arndt, D. S., Baringer, M. O., Eds., *State of the Climate in 2010*,  
601 6. Antarctica. Special supplement to *Bull. Am. Meteorol. Soc.*, 92 (6) 161-172, 2011.

602 Frezzotti, M., Pourchet, M., Onelio, F., Gandolfi, S., Gay, M., Urbini, S., Vincent, C., Becagli,  
603 S., Gragnani, R., Proposito, M., Severi, M., Traversi, R., Udisti, R., and Fily, M.: Spatial and  
604 temporal variability of snow accumulation in East Antarctica from traverse data, *J. Glaciol.*,  
605 51(178), 113-123, 2005.

606 Frieler, K., Clark, P. U., He, F., Buizert, C., Reese, R., Ligtenberg, S.R. M., Van den Broeke,  
607 M. R., Winkelmann, R., and Levermann, A.: Consistent evidence of increasing Antarctic  
608 accumulation with warming, *Nature Climate Change*, 5, 348-352,  
609 doi:10.1038/NCLIMATE2574, 2015.

610 Fujita, K., and Abe, O.: Stable isotopes in daily precipitation at Dome Fuji, East Antarctica,  
611 *Geophys. Res. Lett.*, 33, L18503, doi:10.1029/2006GL026936, 2006.

612 Godfred-Spenning, C. and Simmonds, I.: An analysis of Antarctic Sea-Ice and Extratropical  
613 cyclone associations. *Int. J. Climat.*, 16, 1315-1332, 1996.

614 Gorodetskaya, I.V., N.P.M. Van Lipzig, M. R. Van den Broeke, A. Mangold, W. Boot, and C.  
615 H. Reijmer: Meteorological regimes and accumulation patterns at Utsteinen, Dronning Maud  
616 Land, East Antarctica: Analysis of two contrasting years. *J. Geophys. Res.*, 118, 1-16,  
617 doi:10.1002/jgrd.50177, 2013.

618 Harig, C., and Simons, F. J.: Accelerated West Antarctic ice mass loss continues to outpace  
619 East Antarctic gains. *Earth Planet. Sci. Lett.* 415, 134-141, doi:10.1016/j.epsl.2015.01.029,  
620 2015.

621 Hirasawa, N., Nakamura, H., and Yamanouchi, T.: Abrupt changes in meteorological  
622 conditions observed at an inland Antarctic station in association with wintertime blocking.  
623 *Geophys. Res. Lett.*, 27(13), 1911-1914, 2000.

624 Hirasawa, N., Nakamura, H., Motoyama, H., Hayashi, M., and Yamanouchi, T.: The role of  
625 synoptic-scale features and advection in a prolonged warming and generation of different

626 forms of precipitation at dome Fuji station, Antarctica, following a prominent blocking event,  
627 J. Geophys. Res., 118, 6916-6928, doi:10.1002/jgrd.50532, 2013.

628 Jouzel, J., Vimeux, F., Caillon, N., Delaygue, G., Hoffmann, G., Masson-Delmotte, V., and  
629 Parrenin, F.: Magnitude of isotope/temperature scaling for interpretation of central Antarctic  
630 ice cores, J. Geophysic. Res., 108 (D12), 4361, doi:10.1029/2002JD002677, 2003.

631 Jouzel, J., in: Heinrich Holland and Karl Turekian (Ed.) Treatise on Geochemistry (Second  
632 Edition) 5.8, Elsevier, 213-256, 2014.

633 Karoly, D. J.: Southern Hemisphere circulation features associated with El Nino-Southern  
634 Oscillation events, J. Clim., 2, 1239-1251, 1989.

635 King, J. and Turner, J.: Antarctic Meteorology and Climatology. Cambridge Atmospheric and  
636 Space Sciences Series, Cambridge University Press, Cambridge, 409pp, 1997.

637 Lenaerts, J. T. M., van Meijgaard, E., Van den Broeke, M.R., Ligtenberg, S. R. M., Horwarth,  
638 M., and Isaksson, E.: Recent snowfall anomalies in Dronning Maud Land, East Antarctica, in  
639 a historical and future climate perspective. Geophys. Res. Let., 40, 2684-2688,  
640 doi:10.1002/grl.50559, 2013.

641 Lorius, C., Merlivat, L., Jouzel, J., and Pourchet, M.: A 30,000 years isotope climatic record  
642 from Antarctic ice, Nature, 280, (5724), 644-647, 1979.

643 Marshall, G. J.: Trends in the Southern Annular Mode from observations and reanalyses, J.  
644 Clim., 16, 4134-4143, 2003.

645 Marshall, G. J., : Half-century seasonal relationship between the Southern Annular Mode and  
646 Antarctic temperatures, Int. J. Climatol., 27, 373-383, 2007.

647 Massom, R., Pook, M. J., Comiso, J. C., Adams, N., Turner, J., Lachlan-Cope, T., and Gibson,  
648 T.: Precipitation over the interior East Antarctic ice sheet related to midlatitude blocking-high  
649 activity. J. Climate, 17, 1914-1928, 2004.

650 Masson-Delmotte, V., H. Shugui, A. Ekaykin, J. Jouzel, A. Aristarain, R.T. Bernardo, D. H.  
651 Bromwich, O. Cattani, M. Delmotte, S. Falourd, M. Frezotti, H. Gallée, L. Genoni, A.  
652 Landais, M. Helsen, G. Hoffmann, V. Morgan, H. Motoyama, D. Noone, H. Oerter, J.R.Petit,  
653 A.Royer, R. Ruemura, G. Schmidt, E. Schlosser, J. Simoes, E. Steig, B.Stenni, M. Stievenard,  
654 F. Vimeux, J.W.C. White, 2008. A review of Antarctic surface snow isotopic composition:

655 observations, atmospheric circulation and isotopic modelling. *J. Climate*, 21(13), 3359-3387.  
656 doi 10.1175/2007JCLI2139.1.

657 Monaghan, A. J., Bromwich, D. H., Powers, J. G., Manning, K. W.: The Climate of  
658 McMurdo, Antarctica, Region as Represented by One Year of Forecasts from the Antarctic  
659 Mesoscale Prediction System, *J. Climate*, 18, 1174-1189, 2005.

660 Monaghan, A. J., Bromwich, D. H., Fogt, R. L., Wang, S., Mayewski, P. A., Dixon, D. A.,  
661 Ekaykin, A., Frezzotti, M., Goodwin, I., Isaksson, E., Kaspari, S. D., Morgan, V. I., Oeter, H.,  
662 Van Ommen, T. D., Van der Veen, C. J., and Wen, J.: Insignificant change in Antarctic  
663 snowfall since the International Geophysical Year. *Science*, 313, 827-831, doi:  
664 10.1126/science.1128243, 2006.

665 Nicolas, J. P. and Bromwich, D. H.: Climate of West Antarctica and Influence of Marine Air  
666 Intrusions. *J. Climate*, 24, 49-67. doi:10.1175/2010JCLI3522.1, 2011.

667 Nigro, M. A., Cassano, J. J., and Seefeldt, M. W.: A weather pattern-based approach to  
668 evaluate the Antarctic Mesoscale Prediction System (AMPS) forecasts: Comparison to  
669 automatic weather station observations. *Wea. Forecasting*, 26, 184-198,  
670 doi:10.1175/2010WAF2222444.1, 2011.

671 Nigro, M. A., Cassano, J. J., and Knuth, S. L.: Evaluation of Antarctic Mesoscale Prediction  
672 System (AMPS) cyclone forecasts using infrared satellite imagery. *Antarctic Science*, 24, 183-  
673 192, doi:10.1017/S0954102011000745, 2012.

674 Noone, D., and Simmonds, I.: Implications for the interpretation of ice-core isotope data from  
675 analysis of modelled Antarctic precipitation. *Ann. Glaciol.*, 27, 398-402, 1998.

676 Noone, D., and Simmonds, I.: Associations between  $\delta^{18}\text{O}$  Of water and climate parameters in  
677 a simulation of atmospheric circulation for 1979-95. *J. Clim.*, 15, 3150-3169, 2002.

678 Noone, D., Turner, J., and Mulvaney, R.: Atmospheric signals and characteristics of  
679 accumulation in Dronning Maud Land, Antarctica. *J. Geophysic. Res.*, 104 (D16), 19,191-  
680 19,211, 1999.

681 Nygard, T., Valkonen, T., and Vihma, T.: Antarctic Low-Tropopause Humidity Inversions: 10-  
682 yr Climatology, *J. Climate*, 26, 5205-5219, doi: 10.1175/JCLI-D-12-00446.1, 2013.

683 Powers, J. G., Monaghan, A. J., Cayette, A. M., Bromwich, D. H., Kuo, Y., and Manning, K.  
684 W.: Real-time mesoscale modeling over Antarctica. The Antarctic Mesoscale Prediction  
685 System. *Bull. Am. Meteorol. Soc.*, 84, 1522-1545, 2003.

686 Powers, J. G.: Numerical prediction of an Antarctic severe wind event with the Weather  
687 Research and Forecasting (WRF) Model. *Mon. Wea. Rev.*, 135, 3134-3157, 2007.

688 Powers, J. G., Manning, K. W., Bromwich, D. H., Cassano, J. J., and Cayette, A. M.: A decade  
689 of Antarctic science support through AMPS. *Bull. Amer. Meteor. Soc.*, 93, 1699-1712, 2012.

690 Raphael, M. N.: A zonal wave 3 index for the Southern Hemisphere, *Geophys. Res. Lett.*,  
691 31(23), doi:10.1029/2004GL020365, 2004.

692 Reijmer C. H, Van den Broeke, M. R., and Scheele, M. P.: Air parcel trajectories and snowfall  
693 related to five deep drilling locations in Antarctica based on the ERA-15 dataset, *J. Climate*,  
694 15:1957–1968, 2002.

695 Reijmer, C. H. and van den Broeke, M. R.: Temporal and spatial variability of the surface  
696 mass balance in Dronning Maud Land, Antarctica. *J. Glaciol.*, 49(167), 512-520, 2003.

697 Ritter, F., Steen-Larsen, H. C., Kipfstuhl, J., Orsi, A., Behrens, M., and Masson-Delmotte, V.:  
698 First continuous measurements of water vapor isotopes on the Antarctic Plateau, *Geophys.*  
699 *Res. Abstr.*, 16, EGU2014-9721, 2014.

700 Scarchilli, C., Frezzotti, M., and Ruti, P. M.: Snow precipitation at four ice core sites in East  
701 Antarctica - provenance, seasonality and blocking factors. *Clim. Dyn.*, 37, 2107-2125,  
702 doi:10.1007/s00382-010-0946-4, 2010.

703 Schlosser, E.: Effects of seasonal variability of accumulation on yearly mean  $\delta^{18}\text{O}$  values in  
704 Antarctic snow, *J. Glaciol.* , 45 (151), 463-468, 1999.

705 Schlosser, E., Duda, M. G., Powers, J. G, Manning, K. W.: The precipitation regime of  
706 Dronning Maud Land, Antarctica, derived from AMPS (Antarctic Mesoscale Prediction  
707 System) Archive Data. *J. Geophys. Res.*, 113. D24108, doi: 10.1029/2008JD009968, 2008.

708 Schlosser, E., K. W. Manning, K. W., Powers, J. G., Duda, M. G., Birnbaum, G., and Fujita,  
709 K.: Characteristics of high-precipitation events in Dronning Maud Land, Antarctica. *J.*  
710 *Geophys. Res.*, 115, D14107, doi:10.1029/2009JD013410, 2010.

711 Schlosser, E., Powers, J. G., Duda, M. G., Manning, K. W., Reijmer, C.H., Van den Broeke,  
712 M.: An extreme precipitation event in Dronning Maud Land, Antarctica - a case study using  
713 AMPS (Antarctic Mesoscale Prediction System) archive data. *Polar Research*,  
714 doi:10.1111/j.1751-8369.2010.00164.x, 2010.

715 Schlosser, E., Manning, K. W., Powers, J. G., Gillmeier, S., and Duda, M. G., An extreme  
716 precipitation/warming event in Antarctica – a study with Polar WRF, in preparation, 2016.

717 Sodemann, H, and A Stohl. 2009. Asymmetries in the moisture origin of Antarctic  
718 precipitation. *Geophys.Res. Letters* 36: L22803. doi:10.1029/2009GL040242.

719

720 Sodemann, H., Masson-Delmotte, V., Schwierz, C., Vinther, B. M. and Wernli, H.: Inter-  
721 annual variability of Greenland winter precipitation sources. Part II: Effects of North Atlantic  
722 Oscillation variability on stable isotopes in precipitation, *J. Geophys. Res.*, 113, D12111,  
723 doi:10.1029/2007JD009416, 2008.

724 Schwerdtfeger, W.: *Weather and Climate of the Antarctic*. Elsevier Science Publishers,  
725 Amsterdam-London-New York-Tokyo. 262pp, 1984.

726 Seefeldt, M. W., and Cassano, J. J.: An analysis of low-level jets in the greater Ross Ice Shelf  
727 region based on numerical simulations. *Mon. Wea. Rev.*, **136**, 4188-4205. doi:  
728 10.1175/2007JAMC1442.1, 2008.

729 Seefeldt, M. W., and Cassano, J. J.: A description of the Ross Ice Shelf air stream (RAS)  
730 through the use of self-organizing maps (SOMs). *J. Geophys. Res.*, **117**, D09112.  
731 doi:10.1029/2011JD016857, 2012.

732 Simmonds, I., Keay, K., and Lim, E.: Synoptic activity in the seas around Antarctica. *Mon.*  
733 *Wea. Rev.*, 131, 272-288, 2002.

734 Sinclair, M. R.: Record-high temperatures in the Antarctic – A synoptic case study, *Mon. Wea.*  
735 *Rev.*, 109, 2234- 2242, 1981.

736 Skamarock, W. C., Klemp, J. B., Dudhia, J., Gill, D. O., Barker, D. M., Duda, M. G., Huang,  
737 X., Wang, W, and Powers, J. G.: A description of the Advanced Research WRF Version 3,  
738 NCAR/TN 475+STR, 125 pp., Nat. Cent. for Atmos. Res., Boulder, Co, 2008.



739 Stenni, B., Masson-Delmotte, V., Johnsen, S., Jouzel, J., Longinelli, A., Monnin, E.,  
740 Roethlisberger, R., and Selmo, E.: An Oceanic Cold Reversal During the Last Deglaciation,  
741 *Science*, 293, 2074-2077, 2001.

742 Stenni, B., Masson-Delmotte, V., Selmo, E., Oerter, H., Meyer, H., Roethlisberger, R., Jouzel,  
743 J., Cattani, O., Falourd, S., Fischer, H., Hoffmann, G., Iacumin, P., Johnsen, S. F., Minster, B.,  
744 and Udisti, R.: The deuterium excess records of EPICA Dome C and Dronning Maud Land  
745 ice cores (East Antarctica), *Quat. Scie. Rev.*, 29, 146-159, 2010.

746 Steen-Larsen, H. C. , S. J. Johnson, S. J., Masson-Delmotte, V., Stenni, B., Risi, C.,  
747 Sodemann, H., Balslev-Clausen, D., Blunier, T., Dahl-Jensen, D., Ellehøy, M. D., Falourd, S.,  
748 Grindsted, A., Gkinis, V., Jouzel, J., Popp, T., Sheldon, S., Simonsen, S. B., Sjolte, J.,  
749 Steffensen, J. P., Sperlich, P., Sveinbjörnsdottir, A. E., Vinther, B. M., White, J. W. C.:  
750 Continuous monitoring of summer surface water vapor isotopic composition above the  
751 Greenland Ice Sheet, *Atmos. Chem. Phys.*, 13, 4815-4828, 2013.

752 Suzuki, K., Yamanouchi, T., and Motoyama, H.: Moisture transport to Syowa and Dome Fuji  
753 stations in Antarctica, *J. Geophys. Res.*, 113, D24 114, doi:10.1029/2008JD009794, 2008.

754 Thompson, D. W. J., and J. M. Wallace: Annular modes in the extratropical circulation. Part I:  
755 Month-to-month variability, *J. Climate*, 13, 1000-1016.

756 Trenberth, K. E., and Mo, K. C.: Blocking in the Southern Hemisphere, *Mon. Weather Rev.*,  
757 133, 38-53, 1985.

758 Van Loon, H.: The half-yearly oscillation in middle and high southern latitudes and the  
759 coreless winter. *J. Atmos. Sci.*, 24, 472-486, 1967.

760 Van Loon, H., and Jenne, R. L., The zonal harmonic standing waves in the Southern  
761 Hemisphere, *J. Geophys. Res.*, 77, 992-1003, 1972.

762 Winkelmann, R., Levermann, A., Martin, M. A., and Frieler, K.: Increased future ice  
763 discharge from Antarctica owing to higher snowfall. *Nature*, 492, 239-242, 2012.

764

765

766

767

768 **Figure Captions**

769

770 **Fig. 1**

771 Map of Antarctica indicating Dome C and other important deep-drilling sites in Antarctica

772

773 **Fig. 2**

774 AMPS domains used for model output analysis in this study

775

776 **Fig. 3**

777 a) Mean monthly temperatures for 2009 and 2010 at Dome C AWS

778 b) Daily precipitation and daily mean temperature at Dome C for 2009 and 2010

779

780 **Fig. 4**

781 Monthly precipitation at Dome C a) 2009 and b) 2010, distinguishing three different types of  
782 precipitation: diamond dust, hoar frost, and snowfall

783 Relative frequency of diamond dust, hoar frost, and snowfall for c) 2009 and d) 2010

784 The types were determined from photos of the crystals on the platforms by the Avalanche  
785 Research Institute, Arabba, Italy.

786

787 **Fig. 5**

788 a) 500hPa geopotential height from AMPS archive data (Domain 1) 13.9.2009 00Z

789 (The axis of the upper-level ridge mentioned in the text is marked by a bold black line.)

790 b) 24h-precipitation from AMPS 13.9. 2009 00GMT to 24 GMT

791

792 **Fig. 6**

793 Example for synoptic situation, during which precipitation is observed at Dome C, but not  
794 forecast by WRF in AMPS.

795 a) 500 hPa geopotential height, Domain 2.

796 b) 24h-precipitation total (mm) from AMPS

797

798 **Fig. 7**

799 Mean July- 500hPa geopotential height based on AMPS archive model output for 2009 and  
800 2010.

801

802 **Fig. 8**

803 Mean monthly SAM index for 2009 and 2010 (after Marshall, 2003).

804

805 **Fig. 9**

806 a) Monthly mean Zonal Wave Number 3 (ZW3) index for 2009-2010

807 b) July 2009 500hPa geopotential height anomaly: Mean July 2009 height minus long-term  
808 zonal mean height

809 c) July 2010 500hPa geopotential height anomaly: Mean July 2009 height minus long-term  
810 zonal mean height

811

812

813

814

815

816

817 **Fig. 1**

818

819

820

821

822

823

824

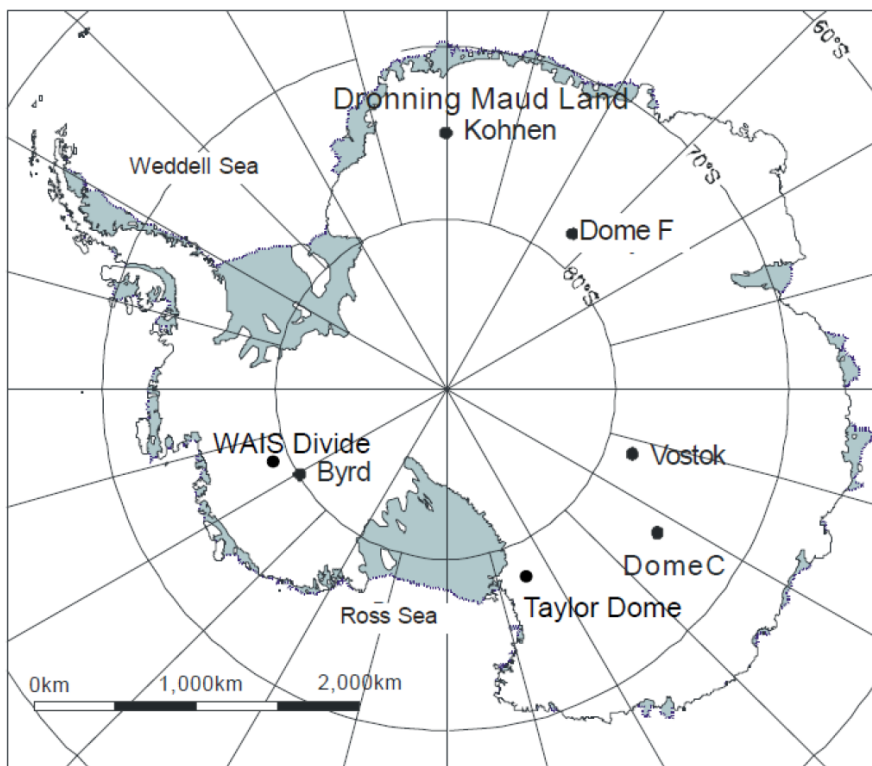
825

826

827

828

829



830

831

832

833

834

835

836

837

838

839

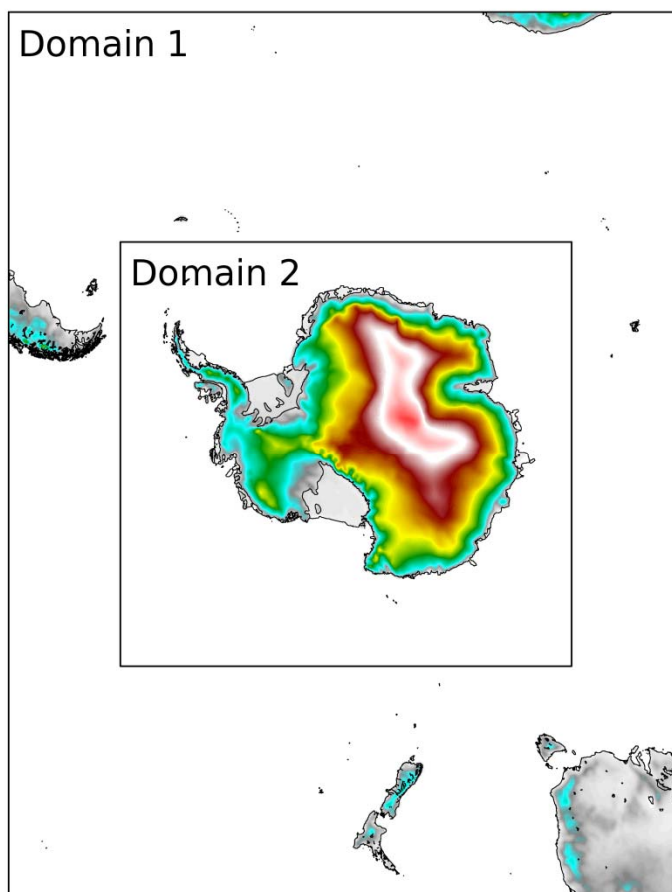
840

841

842

843 **Fig. 2**

844



845

846

847

848

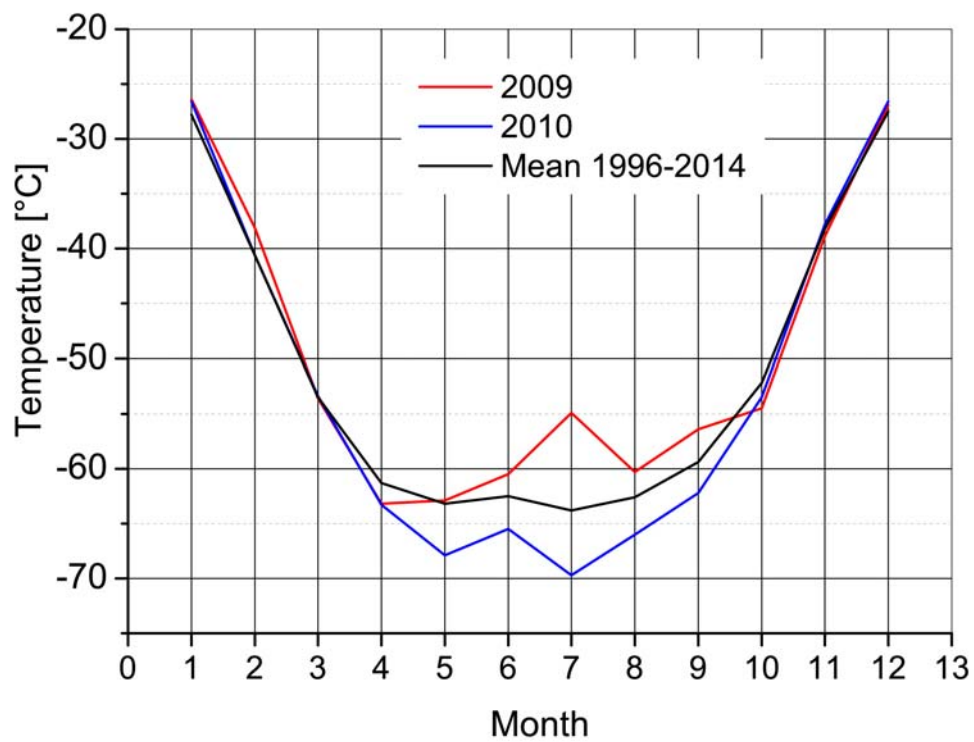
849

850

851 Fig. 3

852

853 a)



854

855

856

857

858

859

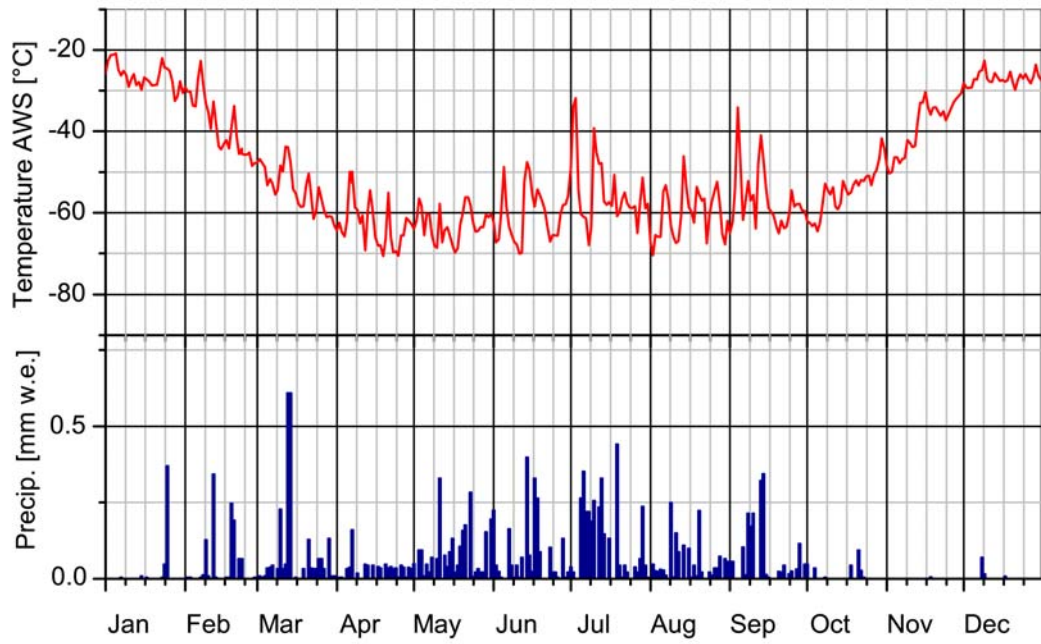
860

861

862

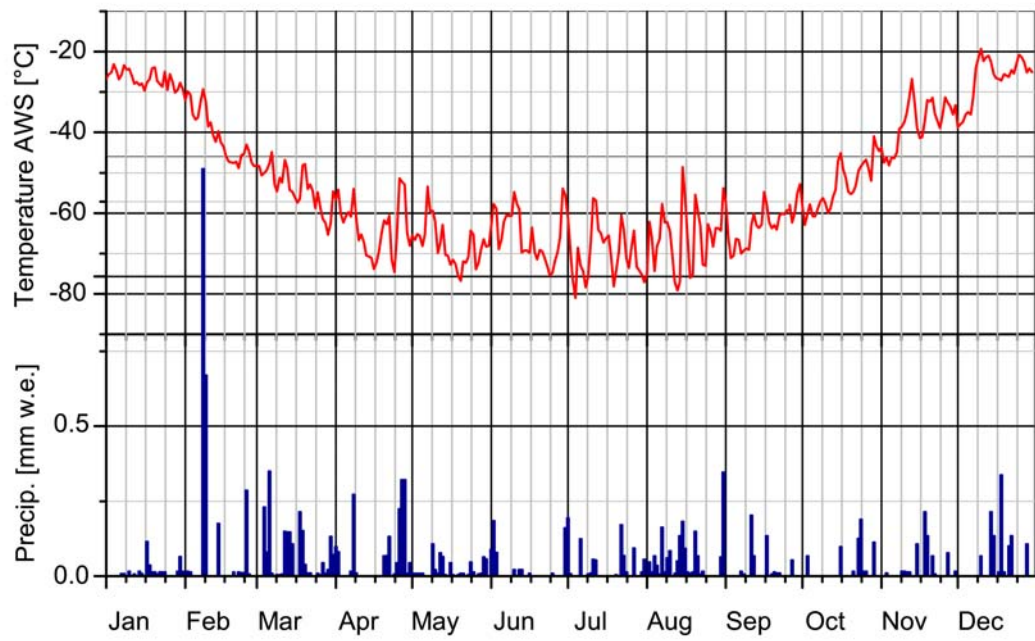
863 b)

864 2009



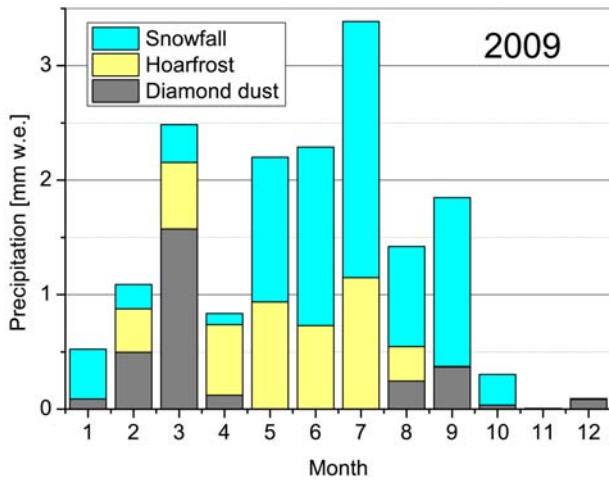
865 2010

866

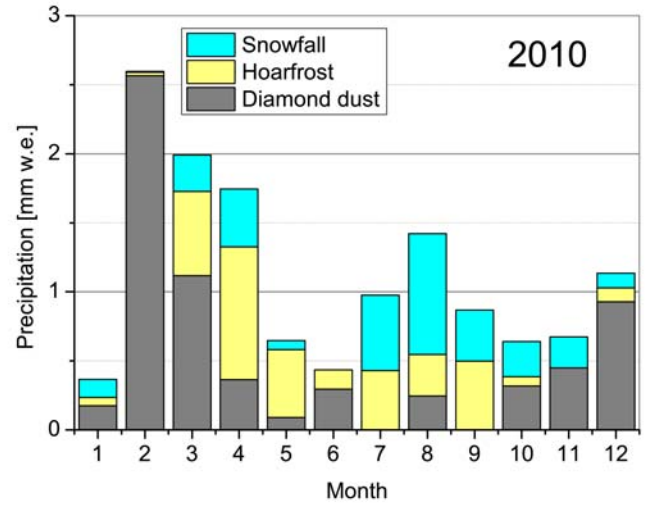


867 **Fig. 4**

868 a)



b)



869

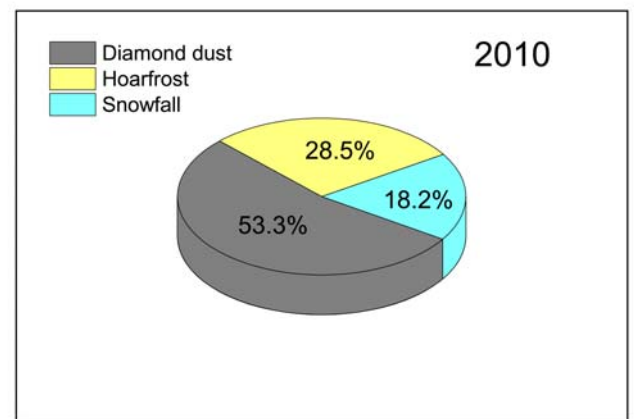
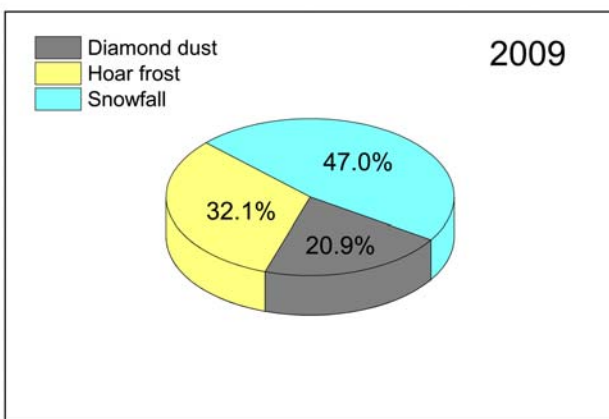
870

871 c)

872

873

d)



874

875

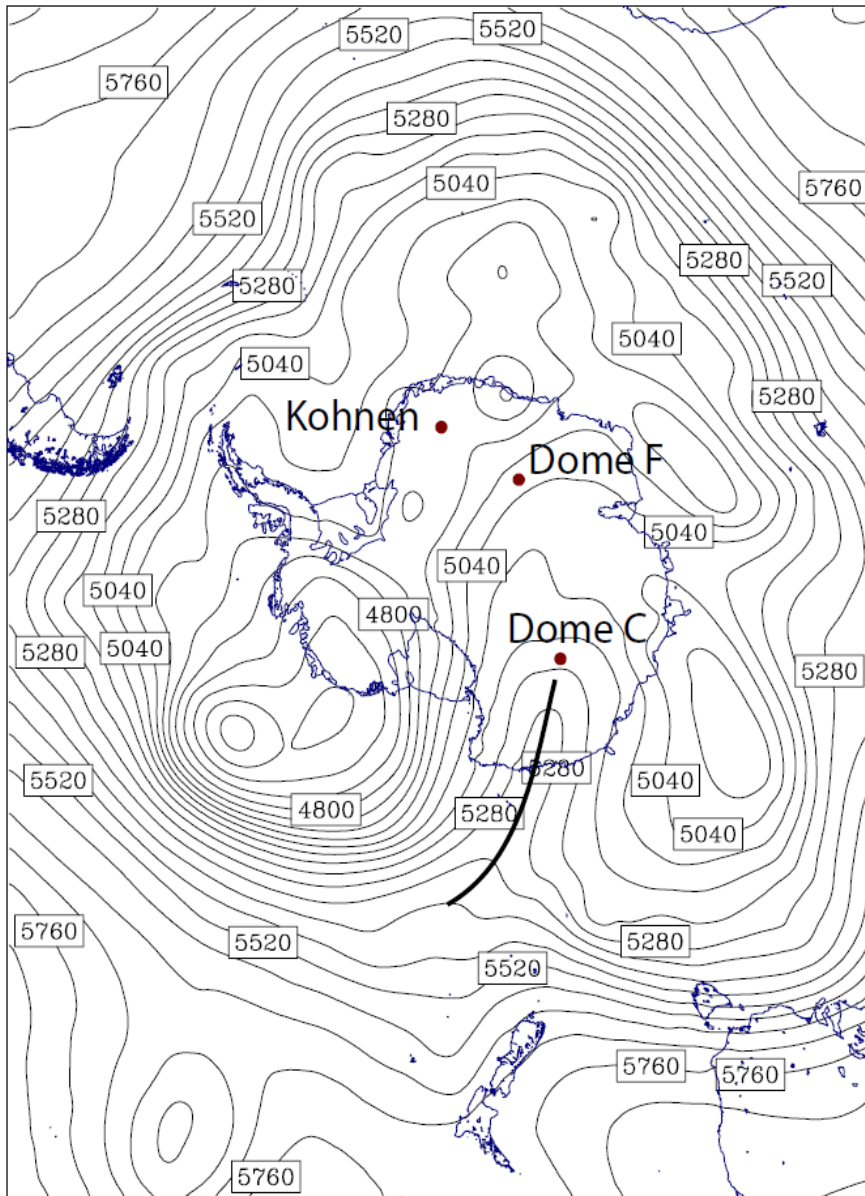
876



877 Fig. 5

878 a)

879



895

896

897

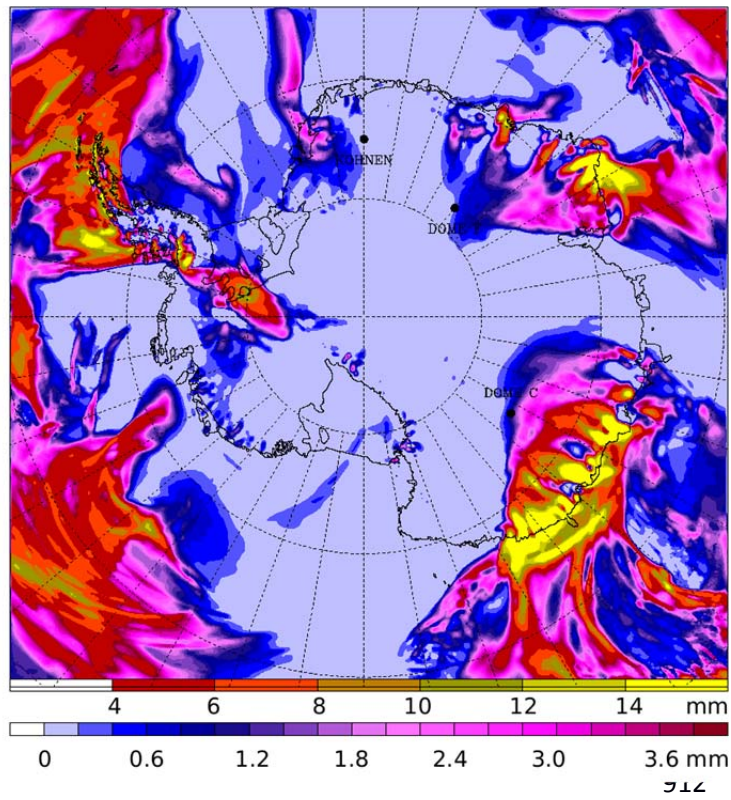
898

899

900

901 **b)**

902



913

914

915

916

917

918

919

920

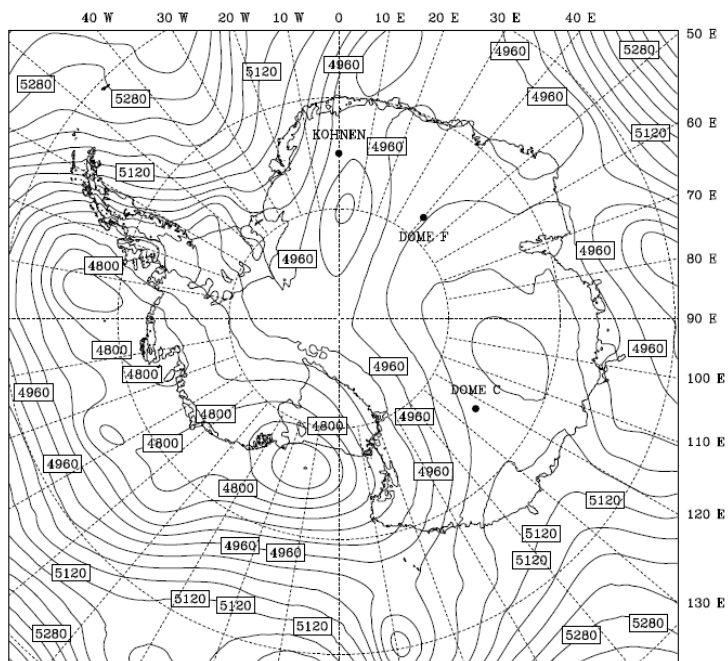
921

922

923 **Fig. 6**

924 **a)**

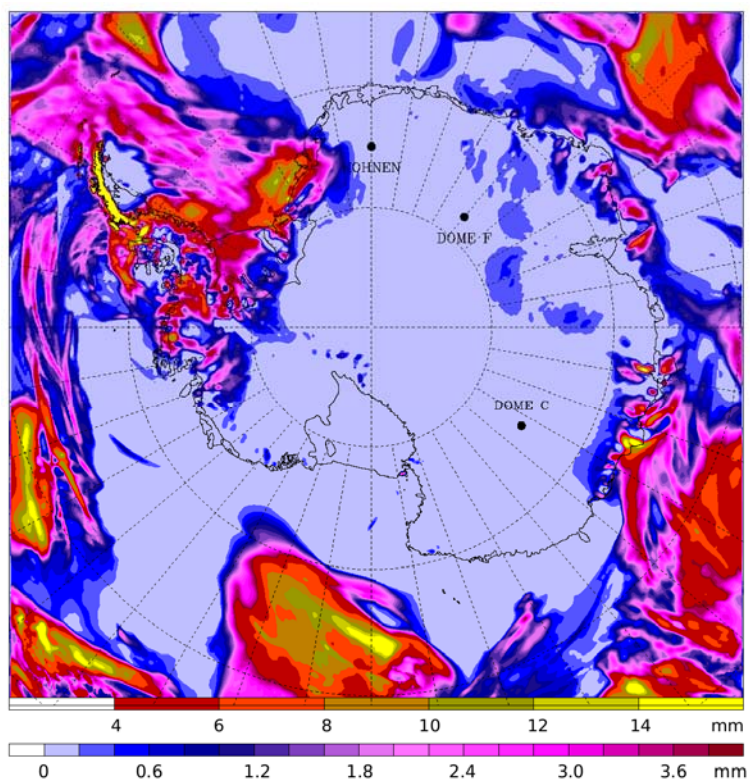
925



935

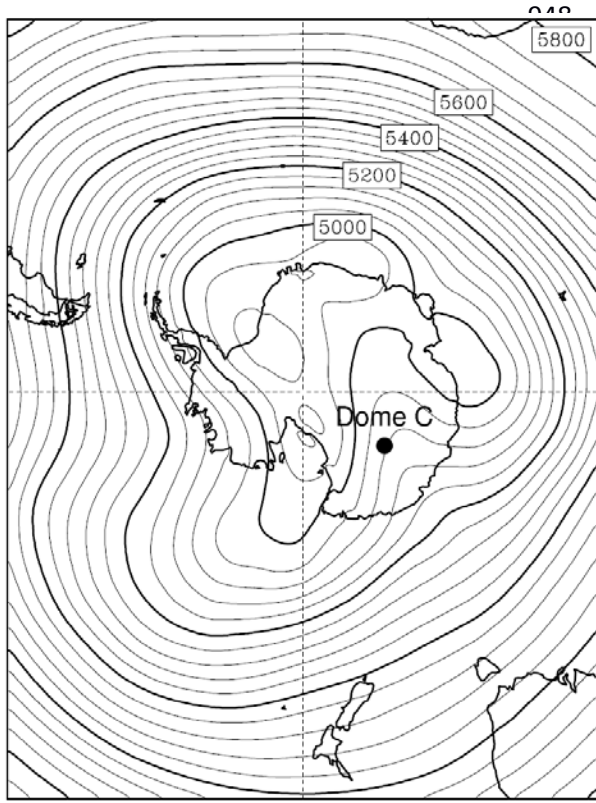
936 **b)**

937

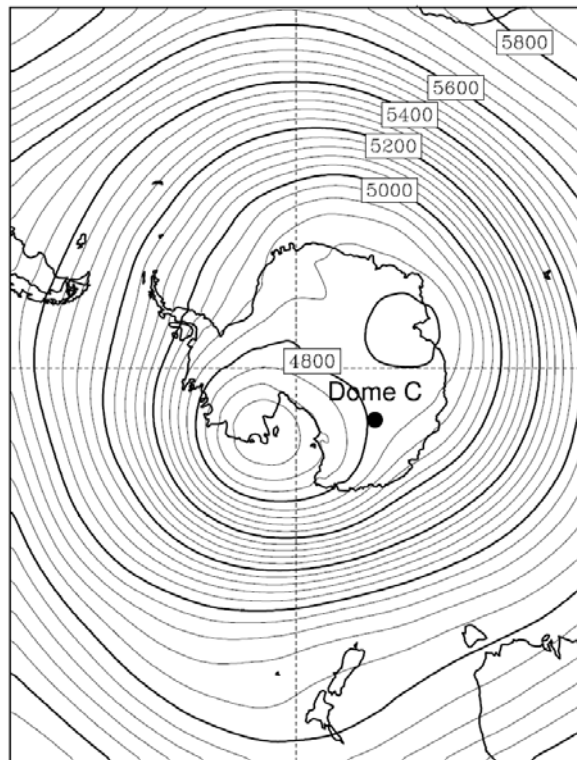


946 **Fig. 7**

947 a) July 2009



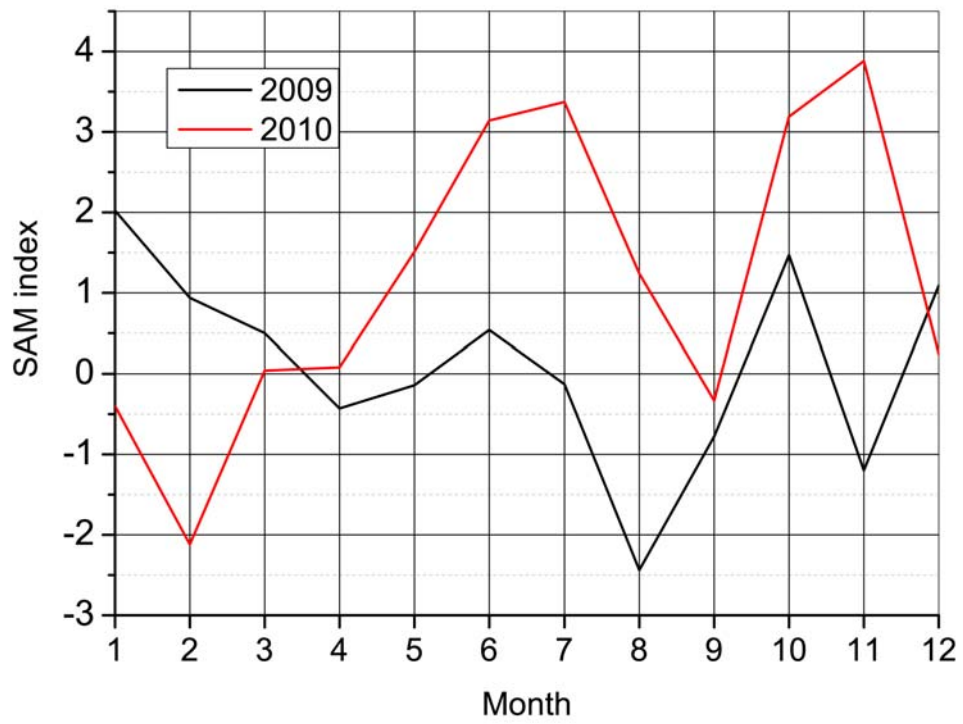
958 b) July 2010



969 **Fig. 8**

970

971



972

973

974

975

976

977

978

979

980

981 **Fig. 9**

982 a)

983

984

985

986

987

988

989

990

991

992

993

994

995

996

997

998

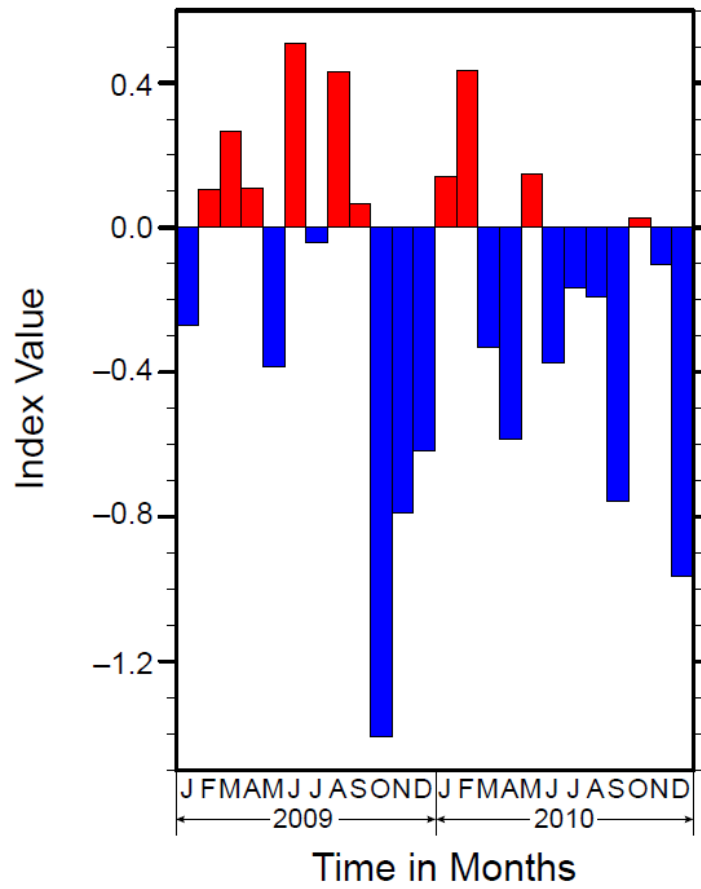
999

1000

1001

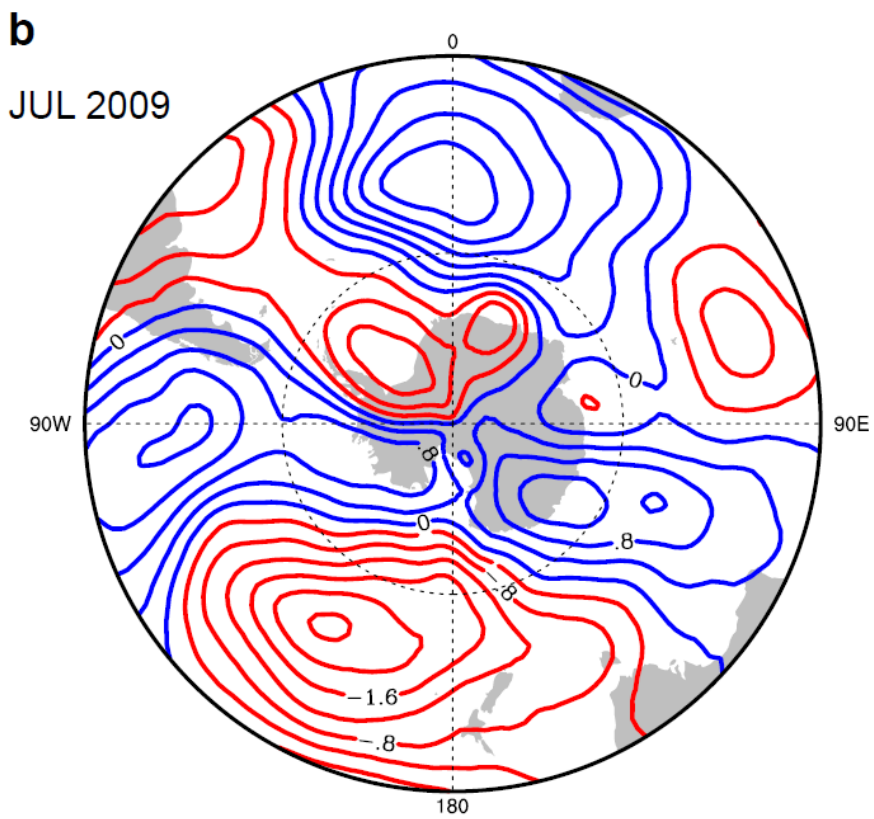
1002

1003



1004 b) 500hPa geopotential height: mean July 2009 minus long-term zonal mean

1005



1016 c) 500hPa geopotential height: mean July 2010 minus long-term zonal mean

1017

